

# A Small Angle Scattering Sensor System for the Characterization of Combustion Generated Particulate

D.A. Feikema<sup>1</sup>

The National Aeronautics and Space Administration  
NASA Glenn Research Center  
21000 Brookpark Road  
Cleveland, OH 44135

and

W. Kim<sup>2</sup>, Y. Sivathanu<sup>3</sup>  
En'Urga Inc.

1291-A, Cumberland Avenue  
West Lafayette, IN 47906

## Abstract

One of the critical issues for the US space program is fire safety of the space station and future launch vehicles. A detailed understanding of the scattering signatures of particulate is essential for the development of a false alarm free fire detection system. This paper describes advanced optical instrumentation developed and applied for fire detection. The system is being designed to determine four important physical properties of disperse fractal aggregates and particulates including size distribution, number density, refractive indices, and fractal dimension. Combustion generated particulate are the primary detection target; however, in order to discriminate from other particulate, non-combustion generated particles should also be characterized. The angular scattering signature is measured and analyzed using two photon optical laser scattering. The Rayleigh-Debye-Gans (R-D-G) scattering theory for disperse fractal aggregates is utilized. The system consists of a pulsed laser module, detection module and data acquisition system and software to analyze the signals. The theory and applications are described.

## I. Introduction

There are two areas within the current NASA program where the proposed instrument can be used. The first is in fire safety system for spacecraft and the space habitats. Characterization of particulate is important to detect the presence of unwanted fires. The second is in characterization of particulate on the moon or mars. There are two key objectives to the proposed work. (1) The first is to utilize these advances in measurement and data interpretation technologies to develop a small angle scattering system that can be used in combustion science studies. (2) A systematic study of the scattering signatures of a wide variety of combustion generated particulate and particulate that are present in the environment with a view of augmenting current fire safety systems utilized in the space station and other future spacecraft.

Obtaining information on the particle size, number density, fractal dimension, and refractive indices is of value in understanding the fundamental composition of the particulates. Black et al. [1996] wrote a comprehensive review of laser based techniques for particle-size measurement. This review details both amplitude dependent and amplitude independent techniques and discusses industrial applications of these methods. Ratio techniques (Chung and Dunn-Rankin, 1996), full-field diffraction measurements (Coil and Farrell, 1995), and forward-scattering techniques (described extensively in Black et al., 1996) are quite prevalent in both laboratory and industrial settings. Forward-scattering (Mie) techniques are utilized

---

<sup>1</sup>Aerospace Research Engineer, Senior Member AIAA, Corresponding Author, email: [douglas.feikema@grc.nasa.gov](mailto:douglas.feikema@grc.nasa.gov)

<sup>2</sup>Scientist, Non AIAA Member, email: [jongmook@enurga.com](mailto:jongmook@enurga.com)

<sup>3</sup>Technical Director, Non AIAA Member, Email: [sivathan@enurga.com](mailto:sivathan@enurga.com)

Copyright © 2007 by NASA GRC and En'Urga Inc., Published by the American Institute of Aeronautics and Astronautics, Inc. with permission.

in a number of commercially available instruments (e.g. Malvern<sup>TM</sup> particle analyzers). However, these techniques are limited to the diagnosis of scattering from spherical particles.

Soot particulate emitted from combustion processes are composed of wispy aggregates consisting of small spherical particles or monomers. Though the small particles satisfy the Rayleigh criteria, the aggregates do not exhibit either Rayleigh or Mie scattering behavior (Dalzell et al., 1970; Magnussen, 1974). Despite the complex geometry of these aggregates, tremendous progress has been made in using fractal based theories for the optical diagnostics of soot particles (Jullien and Botet, 1987; Dobbins and Megaridis, 1991; Koylu and Faeth, 1994).

Dobbins et al. (1990) used light scattering at three angles and aggregate scattering theory to obtain the volume fraction, number of aggregates, aggregate equivalent diameter and radius of gyration in ethylene flames. To obtain these information, the diameter of the primary particle was obtained from TEM and the refractive indices of soot obtained from literature values. Koylu and Faeth (1994) and Farias et al., (1995) showed that if the refractive indices of soot is known, then scattering measurements can be used to infer the aggregate properties. In particular, they showed that the Rayleigh-Debye-Gans/Fractal-Aggregate (RDG-FA) theory agreed with more complete ICP theory of Iskander et al. (1989) in the small angle or Guinier regime. The advantage of using small angle scattering is that the signal strength is the highest at these angles.

The largest sources of uncertainties in their work resulted from a lack of complete knowledge of the refractive indices of soot. There have been numerous studies of the refractive indices of soot (Dalzell and Sarofim, 1969; Lee and Tien, 1981; Habib and Vervisch, 1988, Charalampopolous and Chang, 1988, Choi et al., 1995). The values obtained by different methods varied widely causing interpretation of soot volume fraction by different authors to vary by as much as 30%. In addition, variation of refractive indices with fuel type and temperature (Habib and Vervisch, 1988, Charalampopolous and Chang, 1988) were also noted by a few authors, and not by others (Dalzell and Sarofim, 1969; Lee and Tien, 1981). In addition, multispectral transmittance has been used to simultaneously determine the soot size distribution and the refractive indices in various solid and liquid fuels (Kamiuto, K., 1993). From all these studies, a consensus value for the refractive indices of soot has emerged (Choi et al., 1995), which is very close to that obtained originally by Dalzell and Sarofim (1969).

One of the most exciting developments in deconvolution is the advent of statistical algorithms. It has been recently shown (Vardi and Lee, 1993) for systems with strict positivity constraints (i.e. absorption and scattering are always greater than one and never negative), that a Maximum Likelihood Estimation (MLE) approach based on conditional expectations provides converged solutions. This is a very robust method and was presented before the Royal Statistical Society in 1993. Strict convergence can be proved for a wide array of physical systems ranging from image deblurring to optimal investments (Vardi and Lee, 1993).

Strict convergence implies that the solutions obtained by the method are single valued and minimizes the information distance between the measured and computed observations. The statistical deconvolution algorithm based on MLE method has been used for image reconstruction (Shepp and Vardi, 1982), optimizing investment portfolios, statistical estimation of censored and grouped data, etc.

In microgravity combustion, soot or particulate properties are being studied in a number of projects. In fundamental combustion science studies, soot structure in laminar (Xu et al., 2001) and inverse diffusion flames (Blevins et al., 2001), carbon nanotube formation (Alford et al., 2001) and nano-particle synthesis (Axelbaum et al., 2001) are a few representative sample studies that would benefit from the proposed instrument. In fire safety science, MIST (McKinnon et al., 2001) and SMOKE (Urban et al., 2001) are two experiments that could benefit from obtaining small angle scattering measurements, the former for droplet sizing and the latter for soot morphology.

Current fire detection in spacecraft is based on detection of particulate matter (smoke) using principles of light scattering or ionization. Less than 20 alarms have been recorded by the Space Shuttle during the first 20 years (Friedman and Urban, 2000). Most of these alarms are nuisance alarms caused by particulate stimulus other than smoke or system failures. These nuisance alarms can lead to potentially hazardous situations. Therefore, reviews of spacecraft fire detection have called for instruments that can sense other fire signatures such as temperature rise, combustion gasses, etc. (Friedman and Urban, 2000).

Based on the background, it can be seen that scattering is a feasible method of obtaining particulate properties and utilization of the MLE method is likely to provide the best solution for the various optical parameters. In addition, utilization of multi-spectral data is a reliable method of obtaining refractive indices of soot particles. Finally, if combustion generated particulate can be distinguished readily from nuisance sources, it would greatly benefit the spacecraft safety program.

During the first year of the project, the design of a bench top small angle scattering system was completed. The system was calibrated with 10  $\mu\text{m}$  slit. The system was calibrated with a 514 nm TE cooled diode laser. Based on the calibration, it was ascertained that the system can provide accurate data from 0.05 degrees to 10.5 degrees with an increment of less than 0.1 degrees. This was deemed to be sufficient to discriminate different types of particles.

The first particle that was studied using the system was smoke from an incense stick. The incense stick was burned under a stainless chimney, 7.5 mm in diameter. Scattering intensities were measured at 7 mm above the exit of the chimney. The scattered intensity profile of the incense stick is flat throughout the measured region. This is because the particles are strictly in the Rayleigh regime. The maximum size of the particles is less than 0.3  $\mu\text{m}$ . This is the expected profile for very small particles.

Two modulated diode lasers, one at 532 nm and the other at 670 nm, were purchased and incorporated into the small angle scattering system. Calibration for the lasers were completed, one laser at a time. Additional data obtained from incense sticks showed that both the modulated laser provided correct information from small smoke particles.

## II. Theoretical Considerations

The main objective for understanding the theory is to be able to calculate the theoretical scattering signature from known particle properties. The Rayleigh-Debye-Gans Fractal Aggregate (RDG-FA) theory was used in the forward simulation. An excellent review of the theory has been written by Sorenson (2001). Figure 1 shows a schematic representation of the scattering intensity versus the scattering vector. The RDG-FA theory is briefly explained in the following.  $q$  is the modulus of scattering vector given by the following expression.

$$q = \frac{4\pi \sin(\theta/2)}{\lambda} \quad (2)$$

where  $\lambda$  is the wavelength of light. The aggregate size  $N_c$  at the onset of the power law regime is given by:

$$N_c = k_f \left[ \frac{3D_f/2}{q^2 d_p^2} \right]^{D_f/2} = k_f \left[ \frac{3\lambda^2 D_f}{32\pi^2 \sin^2(\theta/2) d_p^2} \right]^{D_f/2} \quad (3)$$

$k_f$  is the fractal prefactor, and  $d_p$  is the primary particle diameter.  $R_g$ , the radius of gyration can be calculated as:

$$R_g = d_p \left( \frac{N}{k_f} \right)^{1/D_f} \quad (4)$$

The probability density function at the onset of the power regime is given by:

$$p(N) = \frac{\exp\left[-\left(\frac{\ln(N/\bar{N})}{3\sqrt{2}\sigma_g}\right)^2\right]}{3\sqrt{2\pi}\sigma_g S_0 N} \quad (5)$$

where  $\sigma_g$ : geometric standard deviation given by:

$$\sigma_g = \frac{\sqrt{\sum_{i=0}^{N-1} (N_i - \bar{N})^2}}{N-1} \quad (6)$$

$S_0$  is the normalization parameter defined such that  $\sum p(N)$  over all sizes ( $N_0$  to  $N_\infty$ ) is unity.

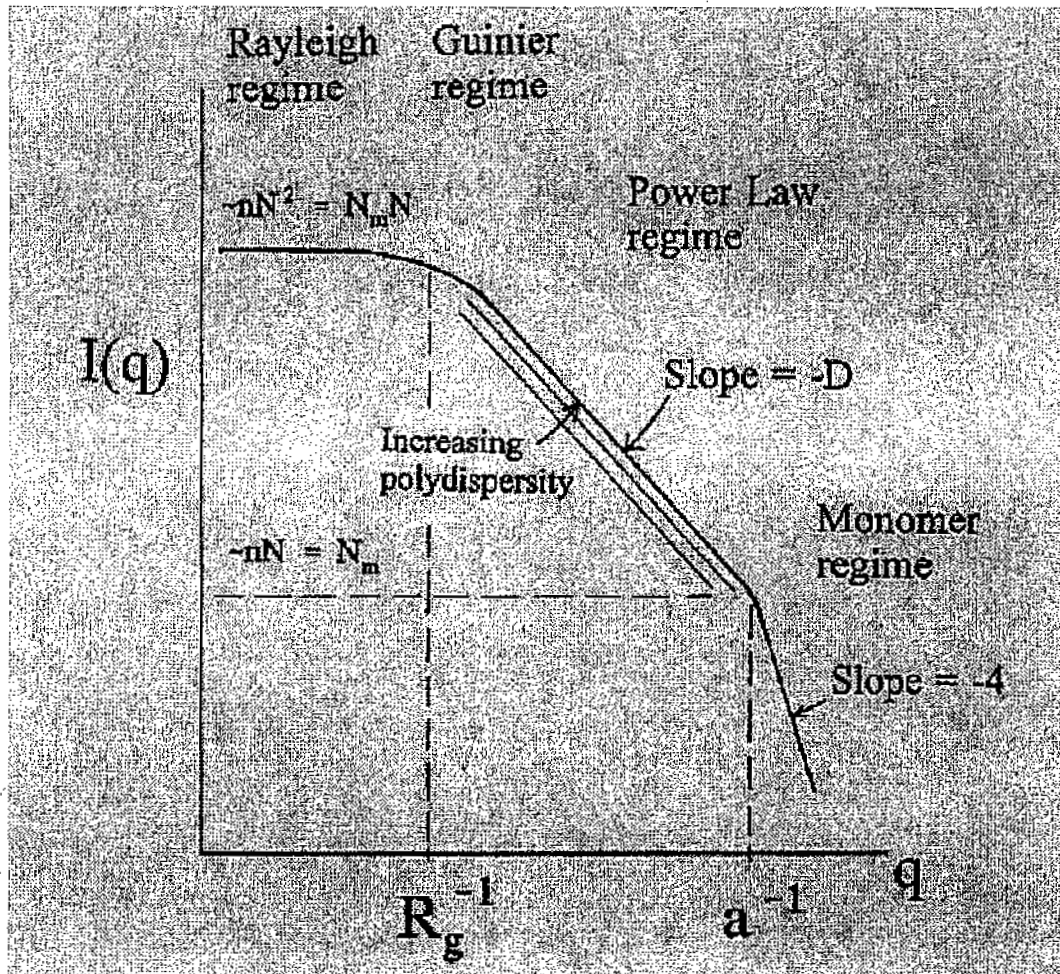


Figure 1 Scattered intensity versus the scattering wave vector illustrating the regimes of the Rayleigh-Debye-Gans/Fractal aggregate theory from Sorenson (2001).

In order to obtain particulate properties from the measured intensities, a maximum likelihood estimation method in conjunction with the Rayleigh-Debye-Gans/Fractal Aggregate theory will be used to deconvolve the measured scattering signals at two wavelengths.

Two key steps are required to convert these voltages to useful information on particle size distribution, number density, refractive indices, and fractal dimension. The first is the calibration of the pixels in the detector array so as to provide absolute intensity values. This will be completed using the non-absorbing DOP as mentioned in the above section. The second step is utilizing these absolute intensities to obtain particulate information.

The scattering cross-sections at small angles (Guinier regime) for fractal aggregates for vertically polarized light can be obtained from the RDG-FA theory as:

$$C_{vv}^a(\theta) = N^2 C_{vv}^p \left[ \exp(-qR_g)^2 / 3 \right] \quad (1)$$

where  $N$  is the number of primary particles in the aggregate,  $qR_g$  is the form factor and  $C_{vv}^p$  is the scattering cross-section of the primary particles given by the following expression.

$$C_{vv}^p = x_p^6 F(m) / k^2 \quad (2)$$

where  $x_p$  is the primary particle diameter,  $k$  is the wave number, and  $F(m)$  is obtained from the refractive indices of the particulate. Eq. (2) assumes that the primary particles are in the Rayleigh regime, which is true for both hydrocarbon soot and silane ash particles.  $F(m)$  is related to the refractive indices as follows:

$$F(m) = \left| (m^2 - 1) / (m^2 + 2) \right|^2 \quad (3)$$

For unpolarized light, the total scattering cross section,  $C_d^a$  can be obtained as:

$$C_d^a = C_{vv}^a (1 + \cos^2 \theta) / 2 \quad (4)$$

For practical cases, the aggregates are polydisperse, and the mean total scattering cross section for unpolarized light is given as:

$$\overline{C}_d^a(\theta) = (1 + \cos^2 \theta) / 2 C_{vv}^p \left[ \exp(-qR_g)^2 / 3 \right] \int_{N=1}^{N_c} N^2 P(N) dN \quad (5)$$

where  $P(N)$  is the probability density function of aggregates.

The absorption cross-section from the polydisperse aggregates is given by:

$$\overline{C}_a^a = 4\pi x_p^3 E(m) / k^2 \int_{N=1}^{N_c} N p(N) dN \quad (6)$$

where  $E(m)$  is obtained from the refractive indices of the particle as:

$$E(m) = \text{Im}((m^2 - 1) / (m^2 + 2)) \quad (7)$$

The extinction cross section is the sum of the absorption and scattering cross-sections.

The measured scattering cross-sections, after calibration using monodisperse non-absorbing aerosol particles, are available at 128 discrete angles and two wavelengths. In addition, the extinction cross-section is also available at two wavelengths.

The number of unknowns in the above set of equations include  $P(N)$ ,  $N$ ,  $R_g$ , and the refractive indices of the particulate. Even using a 50 bin specification for the probability distribution function of sizes, this is an over specified problem. From a purely statistical point of view, the system of equations represented by Eqs. (5) and (6) for the different angles and wavelengths can be solved as a linear inverse problem with positivity constraints (LINPOS). For LINPOS problems, the maximum likelihood estimate (MLE) method provides a converged and unique optimal solution that minimizes the Kullback-Leibler information between the measurements and the predictions using guessed estimates for the unknown optical parameters of the particulate. Details of the maximum likelihood estimation method used for solving LINPOS problems are available in the literature and not provided here.

Utilization of multi-wavelength data provides for two key elements of the proposed system. The first is that multi-spectral data allows the verification of well-known dispersion equations for refractive indices. The second element is that for fire safety, it provides a redundancy in the fire detector, allowing operation even if one of the diode lasers fail.

Other important parameters such as the volume fraction can be easily obtained from the number density and particle size distribution. For example volume fraction can be obtained as:

$$f_v = N_a \frac{\pi}{6} x_p^3 \int_{N=1}^{N=N_c} N p(N) dN \quad (8)$$

where  $N_a$  is the number of aggregates per unit volume.

The above equations were coded by Koylu and Faeth (1994) and the scattering intensity that would be obtained from a typical soot particle generated from an ethylene/air diffusion flames was calculated. The scattering cross-section as a function of angle for a theoretical soot particle is shown in figure 2.

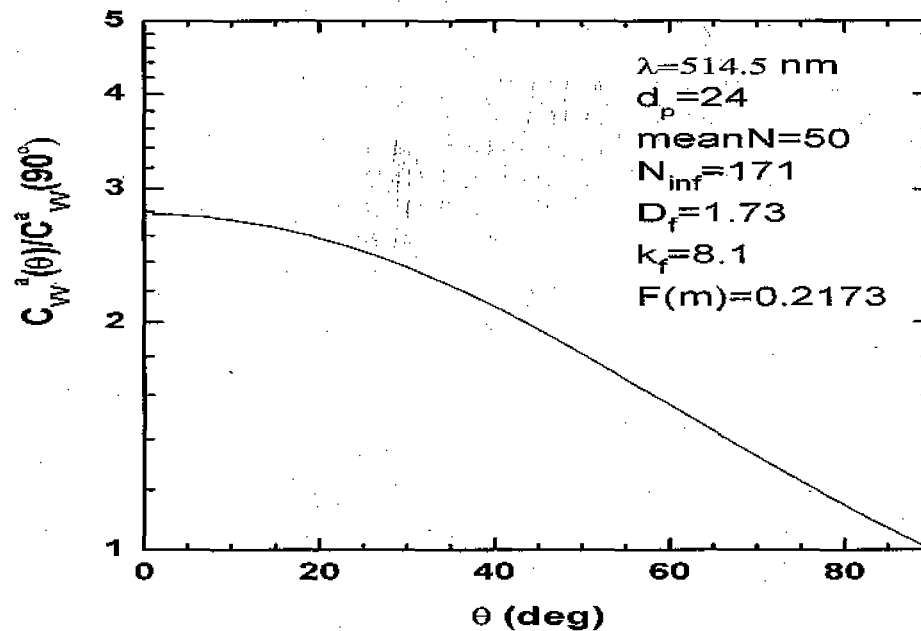


Figure 2. Scattering signatures from a theoretical soot particle in an ethylene/air diffusion flame from Koylu and Faeth (1994).

### III. Hardware Description

The design and fabrication of the two wavelength small angle scattering system (SASS) has been completed. The system was designed using ProEngineer solid model package. The optical design was completed using Zemax Optical Design software.

The mechanical package consists of two separate modules, a laser module and a detector module. The laser module is shown in figure 2. The laser light from two modulated diode lasers, one at 532 nm, and the other at 670 nm, are mixed using a beam splitter and passed through a aperture to the measuring volume. A neutral density filter is placed in front of the 670 nm laser so that the intensity recorded by the linear array from the two lasers are approximately equal. This is essential to enable data collection using a single linear array. The two lasers are modulated at 200 Hz, using a rectangular voltage pulse. A custom printed circuit board (PCB) is used to enable the modulation. The rectangular pulse has a 40% duty cycle (40% high and 60% low). The pulses for both the lasers have a phase difference of 180 degrees. Therefore, both

the lasers are operated out of phase. In addition, the first laser is completely switched off before the second laser is switched on and vice versa.

The detector module is shown in figure 3. The scattered intensity from the measurement volume is collected using a two lens system. The scattered intensity is focused on a linear array, and the data collected using an external computer and data acquisition (DAQ) board. A beam stop is introduced in the detector module to prevent direct laser light from saturating the linear array. Therefore, the middle pixels of the array do not receive any radiation.

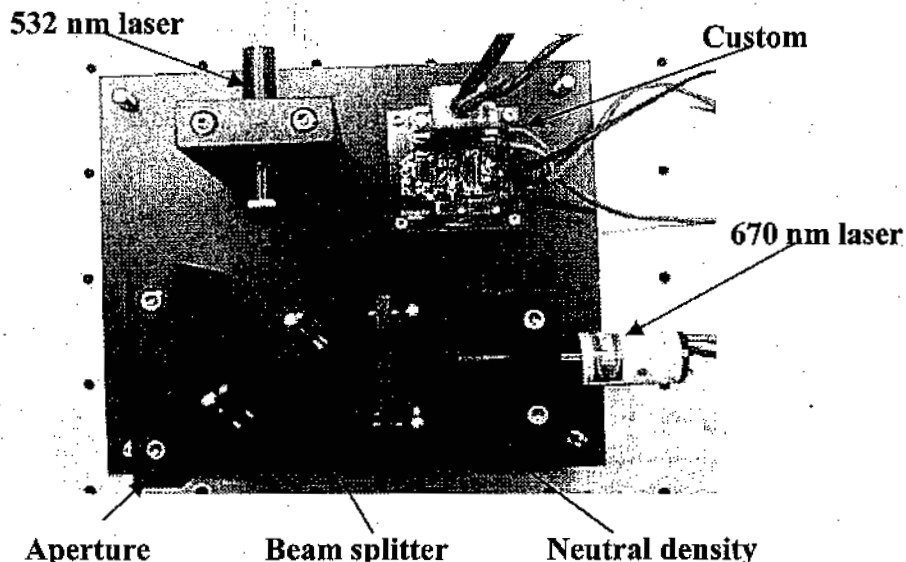


Figure 2. Photograph of the laser module for the SASS.

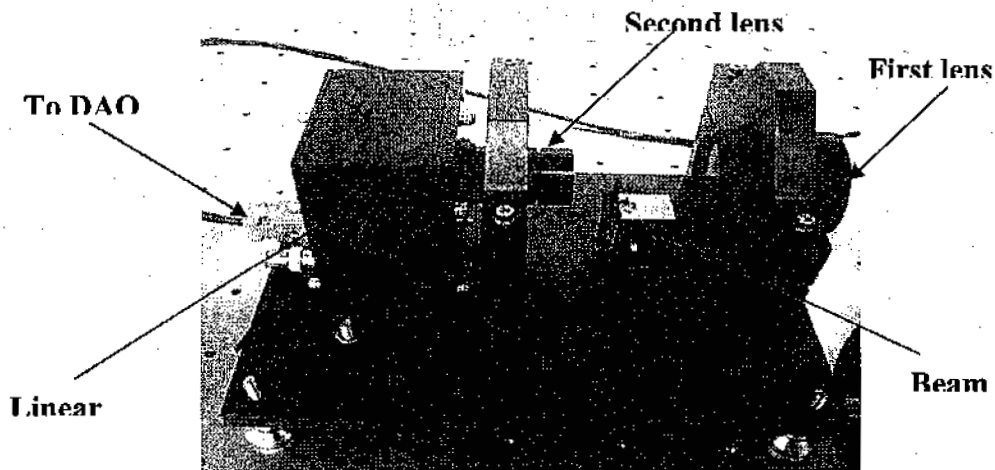


Figure 3. Photograph of the detector/receiver module for the SASS.

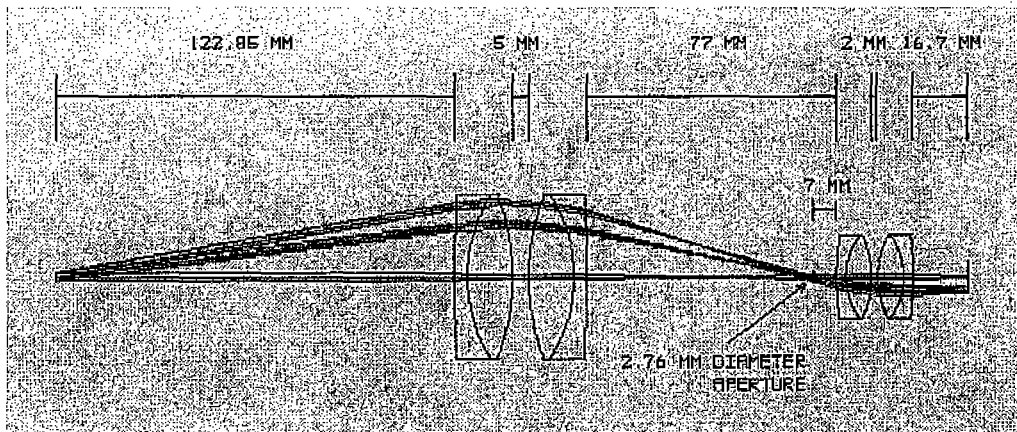


Figure 4. Schematic of the optical design for the SASS.

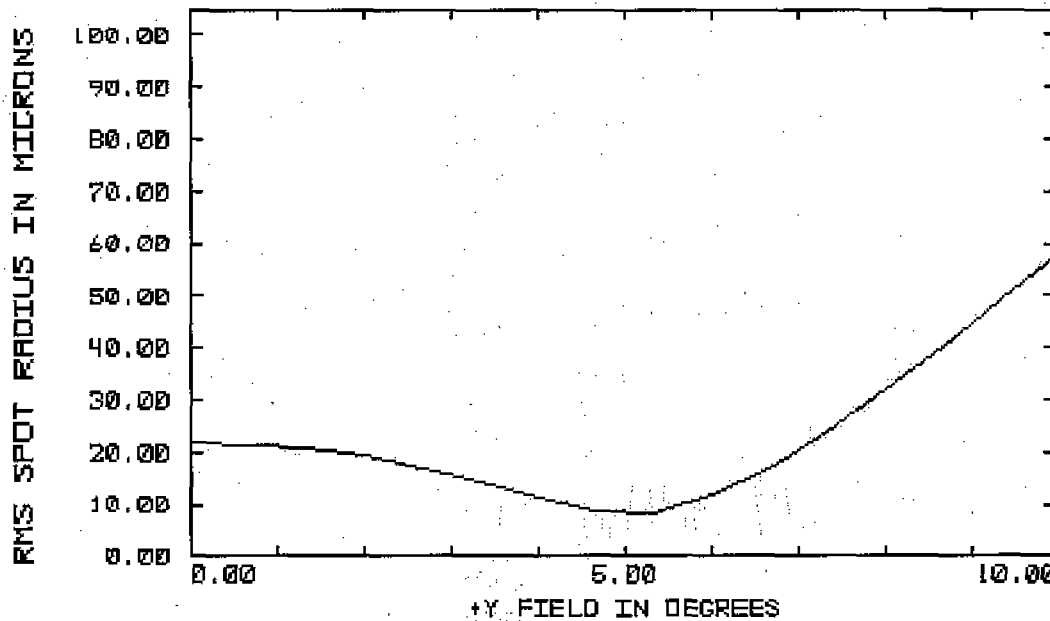


Figure 5. RMS spot radius of the lens system.

A schematic of the optical design for the receiver module is shown in figure 4. The optics for the SASS consists of two lens systems. The first lens system consists of two plano convex lenses (Fourier transform lenses) that collect the scattered intensity from the measuring volume and forms an image at the image plane. The lens is a combination lens made of two materials SF10 and BAFN10 (Edmund Scientific), to avoid chromatic aberration. The focal length of the combination lens is 100 mm. The distance from the front end of the lens to the object plane (measurement volume) is approximately 123 mm. Therefore, using a 50 mm diameter lens, the scattered intensity from approximately 12 degrees. The second set lens system is used to map this image plane onto the linear array detector. The system has two combination plano-convex lenses, made from SF11 and SF5. The focal length of each of the combination lens is 45 mm, with a diameter of 25 mm. The root mean square (RMS) spot radius for the lens is shown in figure 5.



The RMS spot radius of the optical system is less than 25 micrometer up to an angle of 7 degrees. The element size on the linear array is 25 micrometer. The RMS spot radius is computed by tracing several rays through different aperture points and treating the intersections of the rays with the image surface as a random distribution. Typically, 80% of the encircle energy falls within this radius. Therefore, the angular resolution of the system is very good for angles up to 7 degrees. Beyond 7 degrees, the RMS spot radius is higher, implying that the system has only 2 pixel resolution beyond 7 degrees. However, this is still sufficient angular resolution for the deconvolution algorithm.

#### IV. Results and Discussion

The calibration of the SASS was completed using a 10 micron slit. The scattering intensity obtained using the two diode lasers is shown in figure 6. The results show that the system can accurately measure scattered intensities from 0.05 to 11 degrees. Both curves in figure 6 have a constant intensity up to a scattering vector,  $q$ , of  $1 \times 10^3 \text{ cm}^{-1}$  or 10 microns, then the curve begins to bend and the scattered intensity decreases.

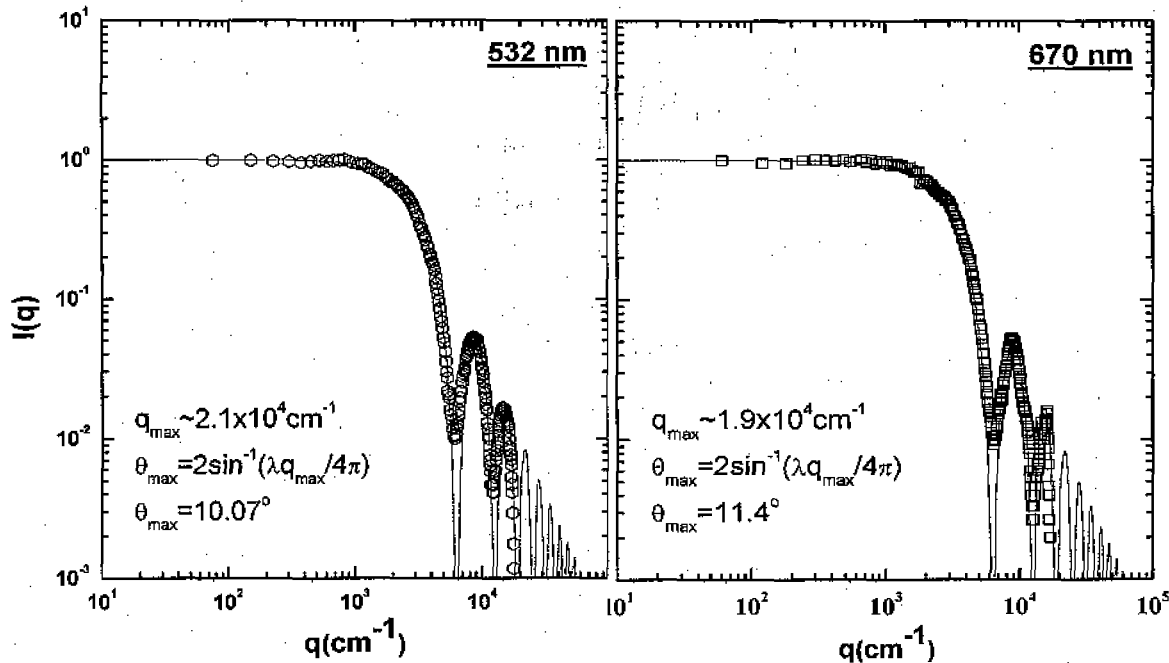


Figure 6. Calibration data for the SASS system.

The first particle that was studied using the system was smoke from an incense stick. The incense stick was burned under a stainless chimney, 7.5 mm in diameter. Scattering intensities were measured at 7 mm above the exit of the chimney. The quantity of smoke issuing from the exit of the chimney was not steady. As a result, the magnitudes of scattering intensities obtained from the experiments were unsteady. It was then decided to decrease the diameter of the tube and place an exhaust fan directly over the tube. For such conditions, we obtained a reasonably stable smoke flow and the amount of smoke doesn't change too much with time. Under the steady state condition, the scattered intensities from the smoke particles were measured using the system. The results obtained from the system are shown in Fig. 7. The intensity profile of the incense stick is flat throughout the measured region. This is because the particles are strictly in the Raleigh regime so

the Rayleigh criteria  $\frac{\pi D_p}{\lambda} < 1$  applies. The maximum possible size of the particles is less than 200 nm (0.2  $\mu\text{m}$ ). This is the expected profile for very small particles. Incense smoke is not an agglomerated particle and are more like individual spherical particles.

The SASS was used to obtain scattering signatures from smoke generated by combustion of PVC, paper, and rubber. The scattering signature obtained from particles generated by burning PVC, insulation material used on electric wires, is shown in figure 8. The intensity is constant up to a scattering angle of  $7^\circ$  at 670 nm and  $8^\circ$  at 532 nm. As shown in figure 1, when the intensity of the scattered signal begins to decrease at a given angle or scattering vector for agglomerated

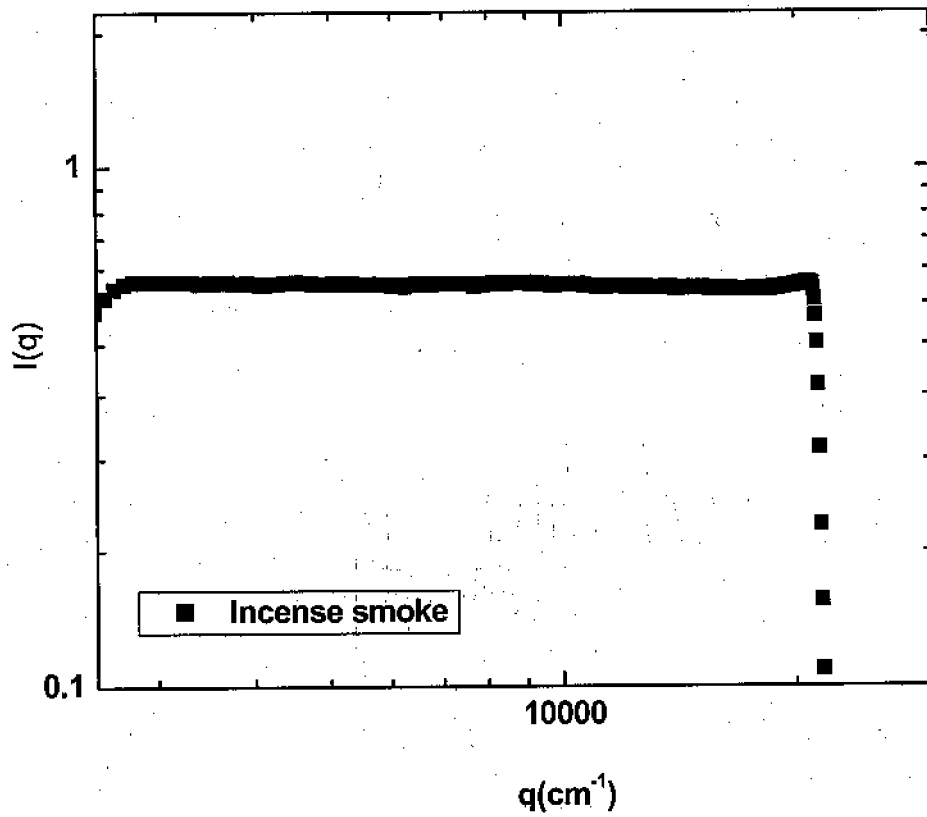


Figure 7 The averaged intensity profile of the incense stick with exhausted system, 670 nm wavelength, broadband detector, photodiode array.

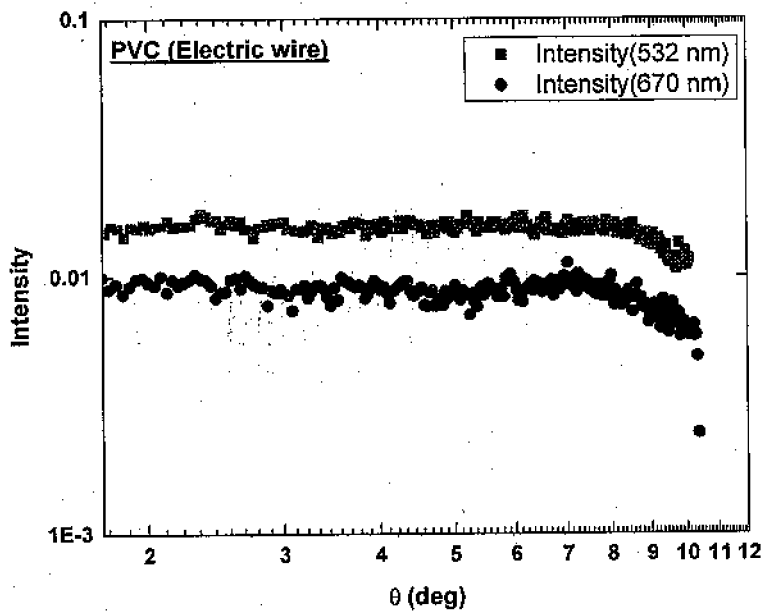


Figure 8. Scattering signatures from particles generated by burning PVC.

particles, the theory predicts this value of the scattering vector to be the radius of gyration. The radius of gyration for the particles shown in figure 8 lie in the range  $0.056$  to  $0.152 \mu\text{m}$ . The scattering signature from particles generated by burning paper is shown in figure 9. The intensity is constant up to a scattering angle of  $8.25^\circ$  at  $670 \text{ nm}$  and  $8^\circ$  at  $532 \text{ nm}$ . The radius of gyration for the particles shown in figure 9 is approximately  $0.06 \mu\text{m}$ .

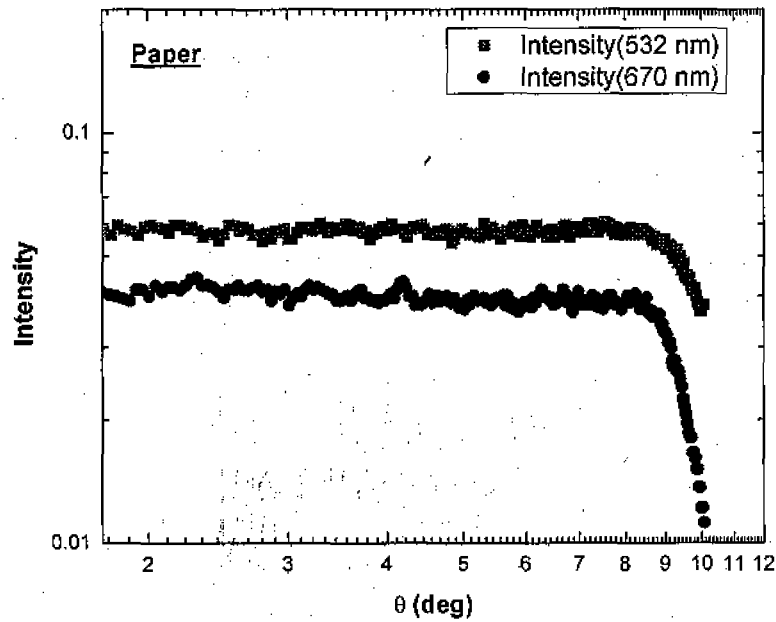


Figure 9. Scattering signatures from particles generated by burning paper.

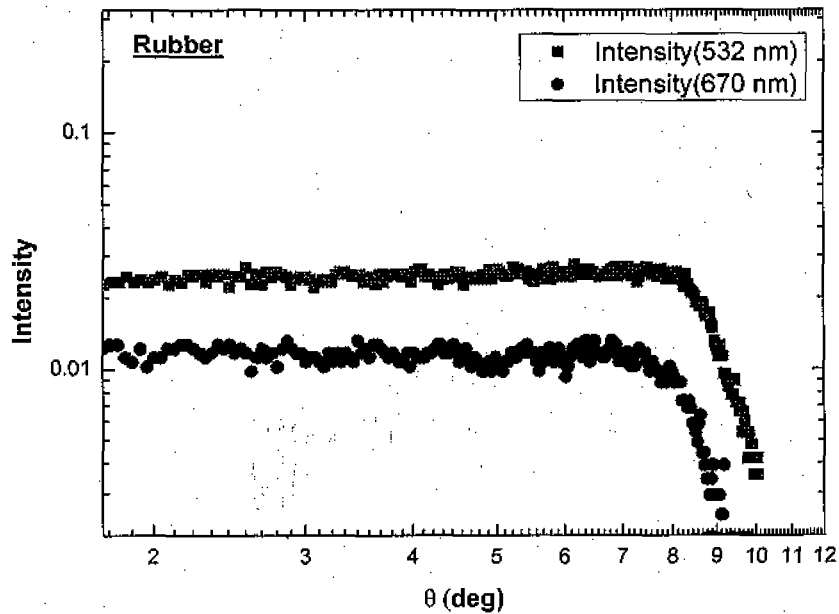


Figure 10. Scattering signatures from particles generated by burning rubber.

The scattering signature from particles generated by burning rubber is shown in figure 10. The intensity is constant up to a scattering angle of  $8.25^\circ$  at 670 nm and  $8^\circ$  at 532 nm. The radius of gyration for the particles shown in figure 10 lie in the range 0.056 to 0.152  $\mu\text{m}$ .

The particles generated by the combustion of all three materials are in the Rayleigh regime. In addition, it is very evident that the particle sizes for rubber, PVC and paper are approximately the same. The combustion generated particulate for the three materials are agglomerated. The mass median diameter for common natural and synthetic materials lie in the range 0.05 to 2.5  $\mu\text{m}$ . The primary particles or monomers generated in hydrocarbon flaming combustion are approximately 20 to 40 nm in size (Buthler and Mulholland (2004), Dod et al. (1985), and Bankston et al. (1978)). Quantitative information on the size and refractive indices of the particles will be provided by the deconvolution algorithm; however, this effort is a work in progress and is not completed at this time.

#### V. Acknowledgements:

This work has been supported by NASA's Microgravity Combustion Science Program which has recently developed into the Fire Prevention, Detection and Suppression Program under NASA contract number NNC04AA40A.

#### VI. References:

- Alford, J. M., Mason, G. R., and Feikema, D. A., 2001, "Formation of Carbon Nanotubes in a Microgravity Environment," *Proceedings of the Sixth International Microgravity Combustion Workshop*, NASA/CP-2001-210826, NASA Glenn Research Center, pp. 293-296.
- Axelbaum, R. L., Kumfer, B. M., Sun, Z., and Chao, B. H., 2001, "Gas-Phase Combustion Synthesis of Nonoxide Nanoparticles in Microgravity," *Proceedings of the Sixth International Microgravity Combustion Workshop*, NASA/CP-2001-210826, NASA Glenn Research Center, pp. 297-300.
- Bankston, C.P., Cassanova, R.A., Powell, E.A., and Zinn, B.T., "Review of Smoke Particulate Properties Data for Natural and Synthetic Materials", NBS-GCR-78-147, 1978.
- Black, D. L., M. Q. McQuay, and M. P. Bonin, 1996, "Laser-based Techniques for Particle-size Measurement: A Review of Sizing Methods and Their Industrial Applications," *Prog. Energy Combust. Sci.*, vol. 22, pp. 267-306.
- Blevins, L. G., Fenandez, M. G., Mulholland, G. W., Davis, R. W., Moore, E. F., Steel, E. B., and Scott, J. H. J., 2001, *Proceedings of the Sixth International Microgravity Combustion Workshop*, NASA/CP-2001-210826, NASA Glenn Research Center, pp. 177-1180.
- Buthler, K.M. and Mulholland, G.W., "Generation and Transport of Smoke Components", *Fire Technology*, 40, pp.149-176, 2004.
- Charalampopoulos, T. T. and Chang, H., 1988, "Insitu Optical Properties of Soot Particles in the Wavelength Range from 340 nm to 600 nm," *Combust. Sci. Tech.*, vol. 59, pp. 401-421.
- Choi, M. Y., Hamins, A., Mullholland, G. W., and Kashiwagi, T., 1995, "Simultaneous Optical Measurement of Soot Volume Fraction and Temperature in Premixed Flames," *Combust. Flame*, vol. 99, pp. 174-186
- Chung, I-P and D. Dunn-Rankin, 1996, "In Situ Light Scattering Measurements of Mainstream and Sidestream Cigarette Smoke," *Aerosol Sci. Tech.*, vol. 24, pp. 85-101.
- Coil, M. A. and P. V. Farrell, 1995, "Full-Field Diffraction Particle Sizing," *Appl. Opt.*, vol. 34, pp. 7771-7786.
- Dalzell, W. H. and Sarofim A. F., 1969, "Optical Constants of Soot and their Application to Heat Flux Calculations," *J. Heat Trans.*, vol. 91, pp. 100-104.
- Dobbins, R. A., and Megaridis, C. M., 1991, "Absorption and Scattering of Light by Polydisperse Aggregates," *Appl. Optics*, vol. 30, pp. 4747-4754.
- Dobbins, R. A., Santoro, R. J., and Semerjian, H. G., 1990, "Analysis of Light Scattering from Soot Using Optical Cross Sections for Aggregates," *Twenty-Third Symposium (International) on Combustion*, The Combustion Institute, Pittsburgh, PA, pp. 1525-1532.
- Dod, R.L., Mowrer, F., Gundel, L.A., Williamson, R.B., and Novakov, T., "Size Fractionation of Black and Organic Particulate Carbon from Fires: Final Report", LBL-20654, Berkeley, CA: Lawrence Berkeley Laboratory, 1985.

- Farias, T. L., Carvalho, M. G., Koylu, U. O., and Faeth, G. M., 1995, "Computational Evaluation of Approximate Rayleigh-Debye-Gans/Fractal-Aggregate Theory for the Absorption and Scattering Properties of Soot," *J. Heat Trans.*, vol. 117, pp. 152-159.
- Freidman and Urban, "Progress in Fire Detection and Suppression Technology for Future Space Missions", AIAA-2000-5251, AIAA Space 2000 Conference and Exposition, September, 2000.
- Greenberg, P.S., Ku, J.C., "Soot Volume Fraction Imaging," *Applied Optics*, Vol. 36, No. 22, pp. 5514-5522, 1997.
- Greenberg, P.S., Ku, J.C., "Soot Volume Fraction Maps for Normal and Reduced Gravity Laminar Acetylene Jet Diffusion Flames," *Combustion and Flame* 108: 227-230, 1997.
- Greenberg, P. S., "Integrated MEMS Particle and Gas Composition Sensors for Intelligent Spacecraft Fire Safety and Environmental Monitoring Systems," "Proceedings of Environmental Sentinels," NASA Johnson Space Center, Houston, TX, September 17-18, 2002.
- Greenberg, P. S. and Hunter, G. W., "MEMS Particulate Sensors for Spacecraft Fire Safety and Environmental Monitoring Applications," Proceedings of the Conference on International Space Station Utilization, AIAA 2001-5047, Port Canaveral, Florida, October 15-17, 2001.
- Habib, Z. G. and Vervisch, P., 1988, "On the Refractive Index of Soot at Flame Temperature," *Combust. Sci. Tech.*, vol. 59, pp. 261-274.
- Iskander, M. R., Chen, H. Y., and Penner, J. E., 1989, "Optical Scattering and Absorption by Branched Chains of Aerosols," *Appl. Optics*, vol. 28, pp. 3083-3091.
- Jullien, R., and Botet, R., 1987, *Aggregation and Fractal Aggregates*, World Scientific Publishing Company, Singapore.
- Kamiuto, K., 1993, "A Multispectral Transmittance Method for Simultaneous Determination of Size Distribution and Optical Dispersion Parameters of Insitu Soot," *JSME International Journal*, vol. 36, pp. 671-676.
- Koylu, U. O., and Faeth, G. M., 1994, "Optical Properties of Overfire Soot in Buoyant Turbulent Diffusion Flames at Long Residence Times," *J. Heat Trans.*, vol. 115, pp. 152-159.
- Lee, S. C. and Tien, C. L., 1981, "Optical Constants of Soot in Hydrocarbon Flames," *Eighteenth Symposium (International) on Combustion*, The Combustion Institute, pp. 1159-1166.
- Magnussen, B. F., 1974, "An Investigation Into the Behavior of Soot in a Turbulent Free Jet  $C_2H_2$ -Flame," *Fifteen Symposium (International) on Combustion*, The Combustion Institute, Pittsburgh, PA, pp. 1415-1425.
- Mckinnon, J. T., Abbud-Madrid, A., Riedel, E. P., Gokoglu, S., Yang, W., Kee, R. J., "The Water-Mist Fire Suppression Experiment: Project Objectives and Hardware Development for the STS-107 Mission," *Proceedings of the Sixth International Microgravity Combustion Workshop*, NASA/CP-2001-210826, NASA Glenn Research Center, pp. 105-108.
- Mulholland, G. W., Yang, J. C., Scott, J. H., and Sivathanu, Y., 2001, 'KISS: Kinetics and Structure of Superagglomerates Produced by Silane and Acetylene,' *Proceedings of the Sixth International Microgravity Combustion Workshop*, NASA/CP-2001-210826, NASA Glenn Research Center, pp. 289-292.
- Nyden, M. R., Vallikul, P., and Sivathanu, Y. R., 1996, "Tomographic Reconstruction of the Moments of Local Probability Density Functions in Turbulent Flow Fields," *J. Quant. Spec. & Rad. Trans.*, vol. 55, pp. 345-356.
- Shepp, L. A. and Vardi, Y., 1982, *IEEE Trans. Med. Imng.*, vol. 1, pp. 113-122.
- Silver, J.A., Kane, D.J., Greenberg, P.S., "Quantitative Species Measurements in Microgravity Flames Using Near-IR Diode Lasers," *Applied Optics*, Vol. 34, No. 15, pp. 2787-2801, 1995.
- Sivathanu, Y. R., and Faeth, G. M., 1990, "Temperature/Soot Volume Correlations in Fuel-rich Region of Buoyant Turbulent Diffusion Flames," *Combust. Flame*, vol. 89, pp. 150-165.
- Sivathanu, Y. R., and Gore, J. P., 1991, "Simultaneous Multiline Emission and Absorption Measurements in Optically Thick Turbulent Flames," *Comb. Sci. Tech.*, vol. 80, pp. 1-21.
- Sivathanu, Y. R., Gore, J. P. and Dolinar, J., 1991, "Transient Scalar Properties of Strongly Radiating Jet Flames," *Combust. Sci. and Tech.*, vol. 76, pp. 45-66.
- Sivathanu, Y. R., and Gore, J. P., 1993, "A Tomographic Method for the Reconstruction of Local Probability Density Functions," *J. Quant. Spec. & Rad. Trans.*, vol. 50, pp. 483-492.
- Sivathanu, Y. R., Hamins, A., Hagwood, C., and Kashiwagi, T., 1995, "Tomographic Reconstruction of the Local PDFs of Soot Volume Fraction and Temperature," *Proceedings of the Joint Technical Meeting of the Central and Western*

*States Sections and the Mexican National Section of the International Combustion Institute and American Flame Research Committee*, pp. 92-97.

- Sivathanu, Y., Hamins, A., Mulholland, G., Kashiwagi, T., and Buch, R., 2001, "Characterization of Particulate from Fires Burning Silicone Fluids," *J. Heat Trans.*, vol. 123, pp. 1093-1097.
- Sivathanu, Y. R., Gore, J. P., Jenssen, J., and Senser, D. W., 1993, "A Study of In situ Specific Absorption Coefficients of Soot Particles in Laminar Flat Flames," *J. Heat Trans.*, vol. 115, pp. 653-658.
- Sivathanu, Y. R., Lim, J., and Joseph, R., 2000, "Statistical Absorption Tomography for Turbulent Flows," *J. of Quant. Spec. and Rad. Trans.*, vol. 68, pp. 611-623.
- Sorenson, C. M., "Light Scattering by Fractal Aggregates: A Review", *Aerosol Science and Technology* 35: 648-687, 2001
- Urban, D. L., Mulholland, G., Yuan, Z. G., Yang, J., and Cleary, T., 2001, "Smoke: Characterization of Smoke Particulate for Spacecraft Fire Detection," *Proceedings of the Sixth International Microgravity Combustion Workshop*, NASA/CP-2001-210826, NASA Glenn Research Center, pp. 401-404.
- Vardi, Y., and Lee, D., 1993, "From Image Deblurring to Optimal Investments: Maximum Likelihood Solutions for Positive Linear Inverse Problems," *J. R. Statist. Soc. B*, vol. 55, pp. 569-612.
- Xu, F., Dai, Z., and Faeth, G. M., 2001, "Suppression of Soot Formation and Shapes of Laminar Diffusion Flames," *Proceedings of the Sixth International Microgravity Combustion Workshop*, NASA/CP-2001-210826, NASA Glenn Research Center, pp. 173-176.